JOC The Journal of Organic Chemistry

Article

pubs.acs.org/joc

DFT Studies on the Mechanism of the Rhodium(III)-Catalyzed C−H Activation of *N*-Phenoxyacetamide

Juan Li* and Zhiping Qiu

Department of Chemistry, Jinan University, Huangpu Road West 601, Guangzhou, Guangdong 510632, People's Republic of China

Supporting Information

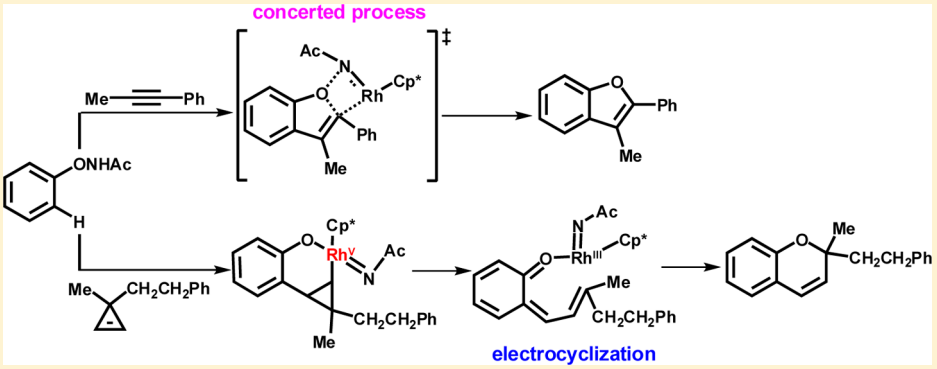

ABSTRACT: A density functional theory (DFT) study has been conducted to elucidate the mechanism of the rhodium(III)-catalyzed C−H activation of *N*-phenoxyacetamide, where the amido component of an internal oxidant serves as a leaving group. The impact of different substrates (alkynes versus cyclopropenes) on the reaction mechanism has been discussed in detail. The pathway for cyclopropene substrate proceeded via a Rh(V) nitrene, while Rh(III) remained unchanged throughout the pathway for alkyne substrate. The C−O bond-forming reductive elimination and O−N bond cleavage steps simultaneously occurred for the alkyne substrate. However, the C−O bond was formed by an electrocyclization from a Rh(III) intermediate for the cyclopropene substrate. The energy profiles for the cyclopropene substrate were accompanied by a change in spin-state because the triplet spin state of a Rh(V) nitrene complex is lower than that of the singlet spin state.

1. INTRODUCTION

Rh-catalyzed directed C−H functionalization reactions represent an atom-economical approach to the construction of heterocyclic compounds, with numerous applications in the organic synthesis of natural products and pharmaceutical molecules.[1] A wide variety of substrates, including alkynes,[2] alkenes,[3] and several other unsaturated molecules,[4] can be used in rhodium(III)-catalyzed C−H functionalization reactions to increase the molecular complexity of the resulting products. However, the need for an external oxidant in most cases to account for the change in oxidation state of the C−H bond, as well as enabling the turnover of the catalyst, represents a significant limitation to the practical application of this approach. For this reason, the use of oxidizing directing groups as internal oxidants has recently emerged as an attractive strategy in C−H activation. The oxidizing directing groups used in these transition-metal-catalyzed C−H functionalization reactions typically contain N−O[5] and N−N[6] bonds.

Several Rh(III)-catalyzed intramolecular C−H functionalization reactions involving the use of *N*-phenoxyacetamides as oxidizing directing groups have recently been reported.[7] For example, Liu et al. reported the unexpected synthesis of a series of valuable benzofuran derivatives via a C−C/C−O bond formation process with the concomitant release of the amido component (Scheme 1).[7a] The results of this particular study were in contrast to the general pattern of C−H functionalization reactions, where the oxy component of the internal oxidant usually serves as a leaving group. In a later study, Wang et al. expanded on the use of *N*-phenoxyacetamides as substrates for coupling with cyclopropenes (Scheme 1),[7b] which represented the first reported example of the use of a cyclopropene as a three-carbon unit in a rhodium(III)-catalyzed C(sp^2)−H bond activation process.

Scheme 1

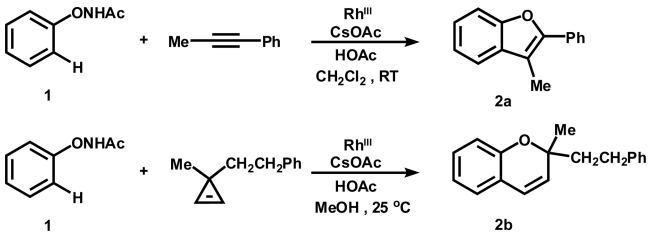

Received: August 14, 2015
Published: October 12, 2015

DOI: 10.1021/acs.joc.5b01895
J. Org. Chem. 2015, 80, 10686−10693

To account for the Rh(III)-catalyzed intramolecular C−H functionalization reactions of *N*-phenoxyacetamides, Liu[7a] and Wang[7b] proposed the reaction mechanisms shown in Schemes 2 and 3, respectively. The general mechanism (Scheme 2) was

Scheme 2

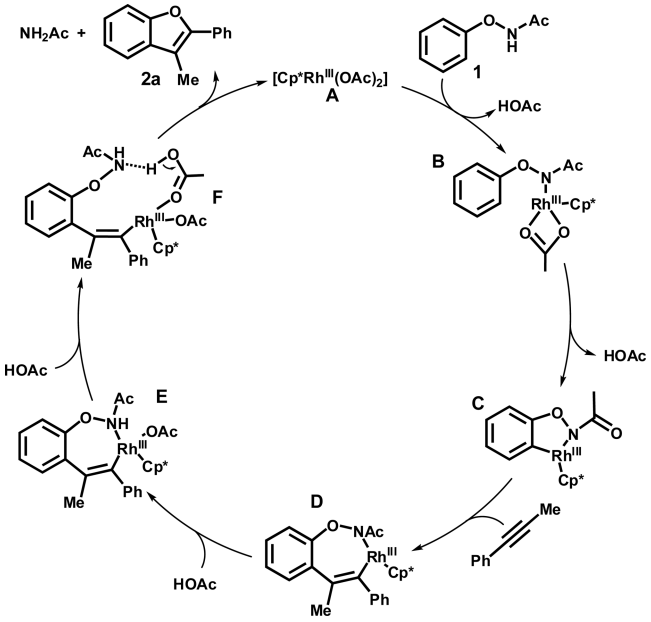

Scheme 3

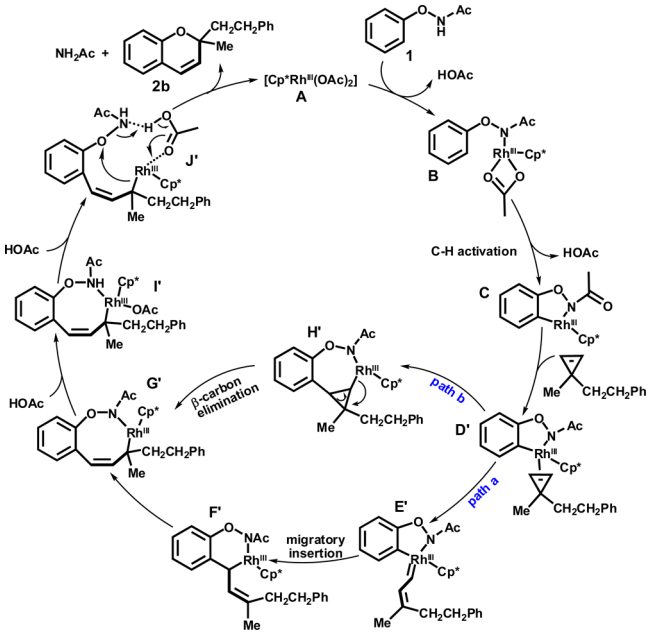

proposed by Liu et al. to account for the synthesis of the benzofuran compounds based on catalytic cycles of C−H activation, alkyne insertion, acetic acid-assisted proton migration, and intramolecular substitution to allow for the formation of the C−O bond. According to the mechanism proposed for the synthesis of 2*H*-chromene (Scheme 3), the first step would be the N−H deprotonation of the *N*-phenoxyacetamide substrate by the Cp*Rh(OAc)$_2$ catalyst **A** to give intermediate **B**. The subsequent cleavage of the ortho C−H bond in **B** would afford the rhodacycle **C**, which could proceed down one of two possible pathways. For path a, the cyclopropene would coordinate to the Rh to generate intermediate **D**′, which would undergo a ring-opening reaction to form the rhodium carbene **E**′. A rhodium carbene migratory insertion reaction would then occur to afford intermediate **F**′, which would be followed by the generation of the eight-membered rhodacyclic intermediate **G**′ through a 1,3-allylic migration. For the alternative path b, the double bond of the cyclopropene substrate would undergo an insertion reaction into the Rh−C bond of **D**′ to give **H**′, which would undergo a β-carbon elimination to form the rhodacyclic intermediate **G**′. Intermediate **G**′ would then undergo an intramolecular substitution reaction, which would be assisted by two molecules of acetic acid to yield the desired 2*H*-chromene product with the regeneration of the catalyst **A**.

However, several important questions concerning the mechanism of the Rh(III)-catalyzed intramolecular C−H functionalization reactions of *N*-phenoxyacetamides remain unanswered. First, the mechanisms proposed in Schemes 2 and 3 do not involve the formation of a Rh(V) intermediate. Given that a Rh(III)/Rh(V) catalytic cycle has been proposed in several other reports,[8] it would be interesting to determine whether a Rh(V) intermediate is involved in the benzofuran and 2*H*-chromene syntheses described above. Second, two different pathways could be used to account for the coupling of the cyclopropene substrates with *N*-phenoxyacetamide according to the mechanism proposed by Wang et al. To eliminate any ambiguity, it would be useful to determine which of these reaction mechanisms is responsible for the reactions of the two different substrates (i.e., alkynes versus cyclopropenes). Furthermore, previously reported theoretical calculations have shown that the triplet spin state is lower in energy than the singlet spin state for the rhodium nitrene complex.[9] The Rh(III)-catalyzed intramolecular C−H functionalization reactions of *N*-phenoxyacetamides could potentially be accompanied by a change in spin-state. In this Article, we have used density functional theory (DFT) calculations to conduct a detailed investigation of the mechanism of the Rh(III)-catalyzed intramolecular C−H functionalization reactions of *N*-phenoxyacetamides using alkynes and cyclopropene as the coupling partners.

2. COMPUTATIONAL DETAILS

The molecular geometries of the complexes were optimized using DFT calculations at the M06 level.[10] Frequency calculations were also performed at the same level of theory to identify all of the stationary points as minima (zero imaginary frequencies) or transition states (one imaginary frequency), as well as the free energies at 298.15 K. An IRC[11] analysis was performed to confirm that all of the stationary points were smoothly connected to each other. The Rh atoms in this analysis were described using the LANL2DZ basis set, including a double-valence basis set with the Hay and Wadt effective core potential.[12] Polarization functions were added for Rh (ζ_f = 1.350).[13] The 6-31G*[14] basis set was used for the other atoms. Single-point energy calculations were conducted using the polarizable continuum model (PCM)[15] to evaluate the solvent effects for all of the gas-phase optimized species. In the PCM calculations, the SDD[16] and 6-311++G** basis sets were used for Rh and all of the other atoms, respectively. All of the calculations were performed using the Gaussian 09 package.[17]

3. RESULTS AND DISCUSSION

Alkynes as Substrates. It appeared reasonable for us to consider the Cp*Rh(OAc)$_2$ fragment as a catalytically

DOI: 10.1021/acs.joc.5b01895
J. Org. Chem. 2015, 80, 10686−10693

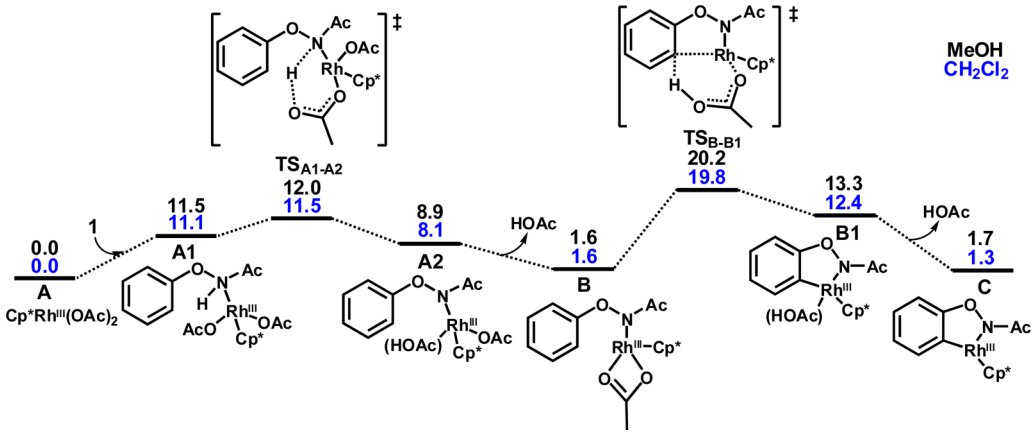

Figure 1. Energy profiles calculated for the coordination, N−H deprotonation, and C−H activation sequence. The solvent-corrected free energies in the PCM model (blue, CH_2Cl_2 as the solvent for the alkyne system; black, MeOH as the solvent for the cyclopropene system) have been given in kcal/mol.

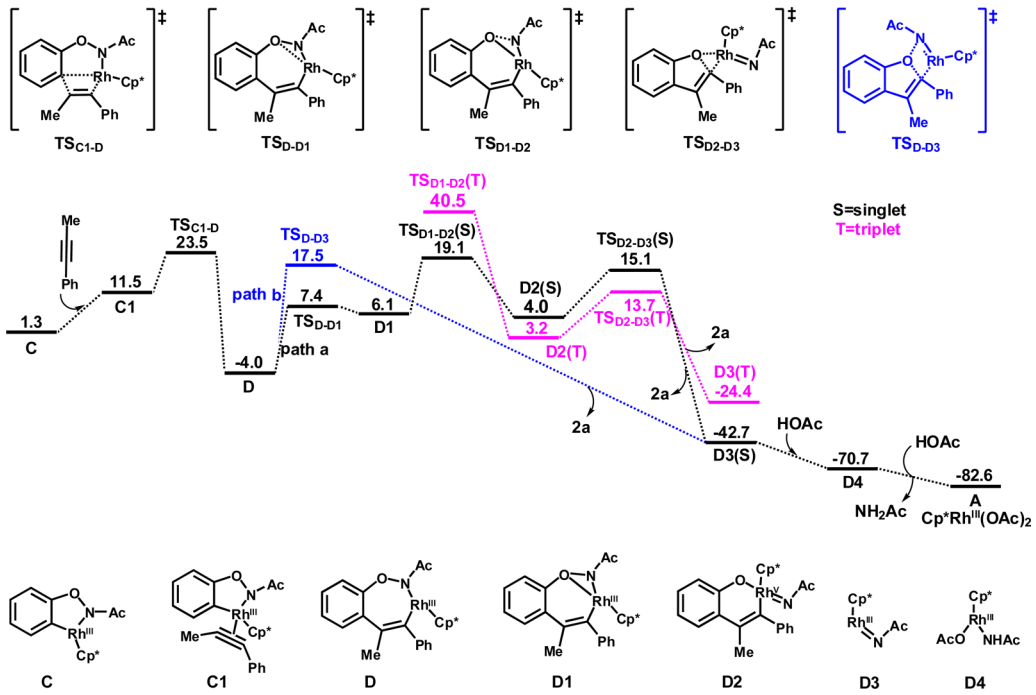

Figure 2. Energy profiles calculated for the processes from intermediate **C** to the benzofuran product and $Cp^*Rh(OAc)_2$ for paths a and b. The solvent-corrected free energies in the PCM model (CH_2Cl_2 as solvent) have been given in kcal/mol.

competent species for $[Cp^*RhCl_2]_2$. It was envisaged that the active species of $Cp^*Rh(OAc)_2$ would coordinate to the *N*-phenoxyacetamide substrate to initiate the reaction, which would be consistent with the results reported by Lin et al.[18] As shown in Figure 1, the reaction would begin with the deprotonation of the amino group, which would be followed by a concerted metalation-deprotonation (CMD) step to give rhodacycle **B1**. The free energy of the CMD transition state was determined to be 19.8 kcal/mol. The alkyne insertion step would begin with the removal of the neutral acetic acid from **B1** to create a vacant coordination site on the Rh(III) center and allow for the coordination of the alkyne substrate, generating **C1**. The subsequent insertion of the alkyne into the Rh−C bond would occur via transition state TS_{C1-D} to give the seven-membered rhodacycle **D** (Figure 2).

Starting from **D**, there are several possible pathways for the formation of the final product. For path a shown in Figure 2, **D** would isomerize to give the bicyclic Rh(III) complex **D1** via a 1,2-rhodium shift with an energy barrier of 11.4 kcal/mol. The subsequent cleavage of the O−N bond in **D1** would afford the rhodium nitrene complex **D2** via transition state TS_{D1-D2}, which would be followed by the formation of a C−O bond through a reductive elimination via TS_{D2-D3} to form the final product **2a** and **D3**. The calculations were performed for TS_{D1-D2}, **D2**, TS_{D2-D3}, and **D3** in both the singlet and the triplet states. The calculations showed that the triplet spin state was lower in energy than the singlet spin state for the rhodium nitrene complex **D2** and TS_{D2-D3}, while the triplet spin state was much higher in energy than the singlet spin state for **D3** and TS_{D1-D2}. These results therefore suggested that inter-system crossing (ISC) processes could occur for TS_{D1-D2} → **D3**.

For the C−O bond-forming reductive elimination and O−N bond cleavage steps, a concerted process (path b) was also

DOI: 10.1021/acs.joc.5b01895
J. Org. Chem. 2015, 80, 10686−10693

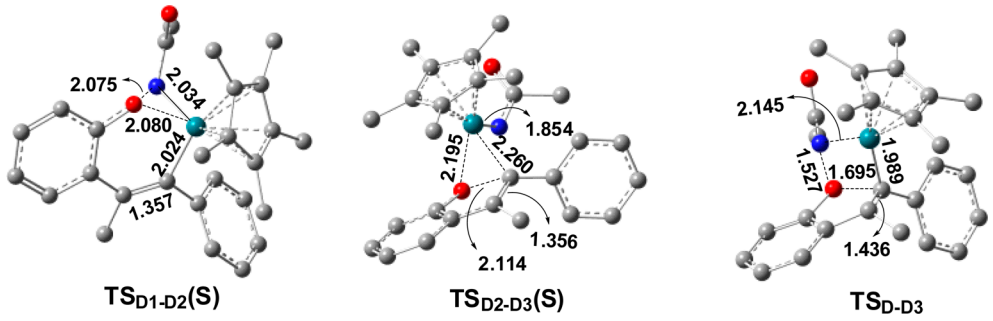

Figure 3. Structures of TS_{D1-D2}, TS_{D2-D3}, and TS_{D-D3} with selected structural parameters. The hydrogen atoms have been omitted for clarity.

possible in which both steps occurred simultaneously. The one-step concerted process via TS_{D-D3} from **D** → **D3**, which had an energy barrier of 21.5 kcal/mol, was more favorable than the three-step process with an energy barrier of 23.1 kcal/mol. As shown in Figure 3, the Rh−C bond distance of TS_{D-D3} (1.989 Å) was even shorter than that of **D** (2.053 Å). This result implied that the π bond of the double bond stabilized TS_{D-D3}, although it was formed in a concerted fashion. To demonstrate the influence of the π bond of the double bond, we replaced it in TS_{D-D3} with a single bond and found the concerted transition state could not be optimized. Finally, a metathesis reaction would occur between H and the two HOAc groups to regenerate the catalyst Cp*Rh(OAc)$_2$. On the basis of the results shown in Figures 1 and 2, it is clear that the transition state for the alkyne insertion is rate-determining for the whole catalytic cycle. The overall energy barrier for this process was calculated to be 23.5 kcal/mol.

As shown in Scheme 4, the C−O bond reductive elimination could occur from **E1**. However, transition state TS_{E1-D4} had a

Scheme 4

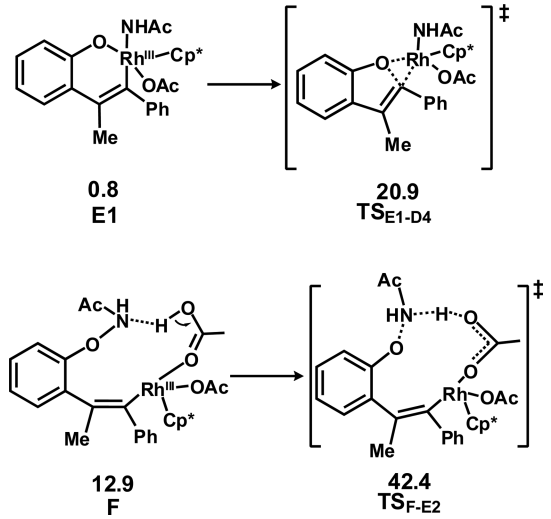

higher energy barrier than **D** (24.9 kcal/mol), which indicated that the pathway would be impossible. In addition, we calculated the energy profile on the basis of the proposed mechanism shown in Scheme 2. Unfortunately, our attempts to locate a transition state for **F** → **2a** + **A** failed, and we were only able to obtain TS_{F-E2} (Scheme 4). The transition state TS_{F-E2} was calculated to have a very high energy barrier of 46.4 kcal/mol relative to **D**. According to our analysis, the transition state for **F** → **2a** + **A** would be too high in energy to be found, which indicated that the pathway shown in Scheme 2 should be impossible.

Furthermore, the alkyne substrate could insert into the Rh−N bond via TS_{C1-D5} to form **D5** (Scheme 5). However, the relative energy of TS_{C1-D5} (30.8 kcal/mol) was found to be higher than that of TS_{C1-D} (23.5 kcal/mol), which indicated that this pathway could be ruled out. To develop a better understanding of the observed regioselectivity, we calculated the alkyne insertion step to form **D6** (Scheme 5), where the metal-bonded carbon forms a bond with the phenyl-substituted carbon of MeC≡CPh. This insertion mode was less favorable than the alternative mode leading to the formation of **D**, where the metal-bonded carbon forms a bond with the methyl-substituted carbon of MeC≡CPh. The result of this calculation was therefore consistent with the experimentally observed regioselectivity.[7a]

Cyclopropenes as Substrates. For computational simplicity, the Cp*Rh(OPiv)$_2$ catalyst was modeled by Cp*Rh(OAc)$_2$. Figures 1 and 4 showed the energy profiles that were calculated for the proposed mechanism in Scheme 3. The initial formation of rhodacycle **C** would be achieved through the deprotonation of the amino group followed by the CMD steps. The subsequent coordination of cyclopropene to the Rh center would lead to the formation of intermediate **D′**, which could proceed down one of two possible pathways (i.e., path a or b). In path a (Figure 4), the ring opening of intermediate **D′** would occur via transition state $TS_{D'-E'}$ to form rhodium carbene **E′** with an energy barrier of 17.1 kcal/mol. The subsequent migratory insertion of the rhodium carbene would occur via $TS_{E'-F'}$ to give intermediate **F′** with a very small energy barrier of 1.5 kcal/mol. Intermediate **F′** would then undergo a 1,3-allylic migration to afford the eight-membered rhodacyclic intermediate **G′**. For the alternative path b, the double bond of the cyclopropene would initially insert into the Rh−C bond of **D′** to give **H′** with an energy barrier of 5.6 kcal/mol. A subsequent β-carbon elimination from **H′** via transition state $TS_{H'-G'}$ would afford the eight-membered rhodacyclic intermediate **G′** with a high energy barrier of 49.0 kcal/mol. The energy barriers for **A** → **G′** for paths a and b were calculated to be 29.9 and 49.0 kcal/mol, which appeared to be too high to allow for the coupling reaction to occur under the experimental conditions.[7b] In the following text, we have presented an alternative mechanism (path c) that is energetically feasible.

Figure 5 shows the energy profiles for **C** → **A** based on path c. The **C** → **H′** step in path c is the same as that shown in path b. From complex **H′**, the formation of a Rh−O bond would afford intermediate **K′** with an energy barrier of 8.1 kcal/mol. The subsequent cleavage of the O−N bond in **K′** would lead to the formation of the Rh(V) nitrene complex **L′** via transition

DOI: 10.1021/acs.joc.5b01895
J. Org. Chem. 2015, 80, 10686−10693

Scheme 5

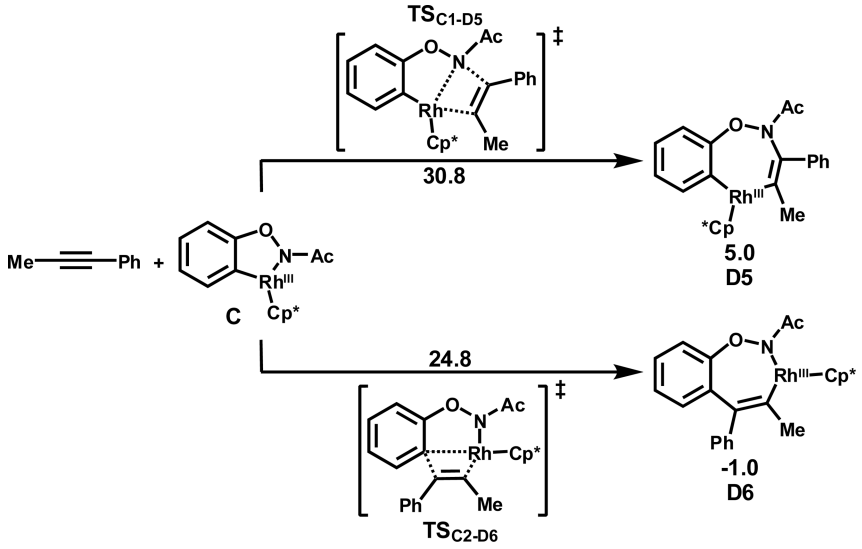

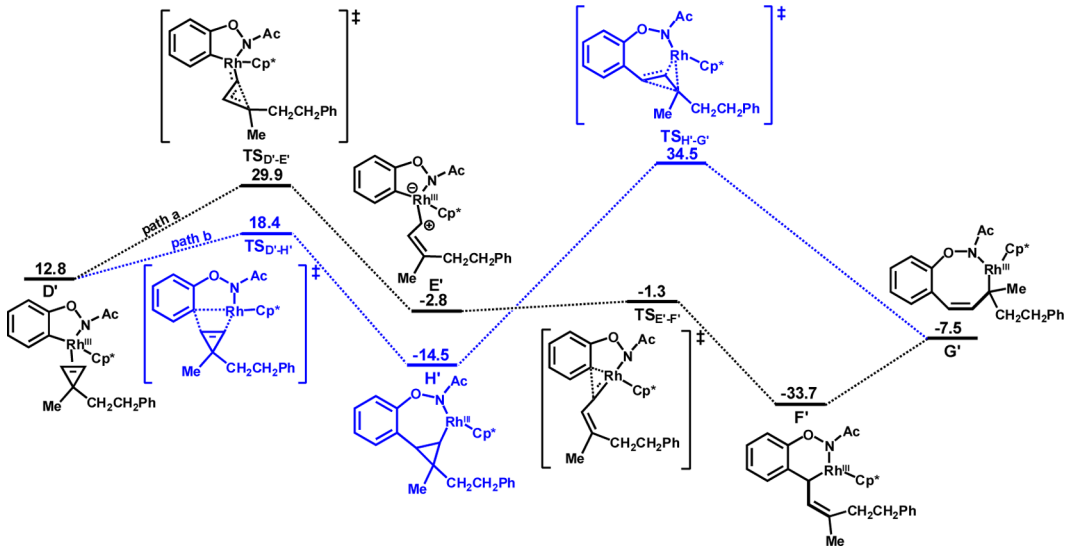

Figure 4. Energy profiles calculated for **D′** → **G′** based on paths a and b. The solvent-corrected free energies in the PCM model (MeOH as solvent) have been given in kcal/mol.

state $\mathbf{TS_{K'-L'}}$, which would be followed by a ring-opening step via transition state $\mathbf{TS_{L'-M'}}$ to form the Rh(III) intermediate **M′**. The subsequent formation of a C−O bond through an electrocyclization mechanism would give the final product **2b** and **D3**. The calculations were performed for $\mathbf{TS_{K'-L'}}$, **L′**, $\mathbf{TS_{L'-M'}}$, and **M′** in both the singlet and the triplet states. The results of the calculations showed that the triplet spin state was lower in energy than the singlet spin state for **L′** and $\mathbf{TS_{L'-M'}}$, while the triplet spin state was much higher in energy than the singlet spin state for $\mathbf{TS_{K'-L'}}$ and **M′**. Therefore, the ISC processes should occur for $\mathbf{TS_{K'-L'}}$ → **M′**. **L′(S)** and **L′(T)** were close in energy because the π interaction of the rhodium with the nitrene nitrogen atom stabilized the singlet state.[19] The Rh−N distance of the rhodium-nitrene complex **L′** in its singlet and triplet states is 1.860 and 1.964 Å, respectively. In **L′(T)**, the spin densities mainly reside on the N (1.039) atom and rhodacycle (0.764) because of the total spin densities of these being 1.803. Finally, the protonation of **D3** under the assistance of two HOAc molecules would allow for the regeneration of the catalyst **A**. The overall free energy barrier for path c was calculated to be 23.4 kcal/mol, which corresponded to the energy of $\mathbf{TS_{K'-L'}}$ relative to **H′**. A comparison of the energy profiles shown in Figures 4 and 5 shows that paths a and b, which are based on the mechanism proposed by Wang et al. (Figure 4), are energetically less favorable than our newly proposed mechanism shown as path c (Figure 5).

It would not be possible for the formation of Rh(V) intermediate **M1′** through the ring opening of **L′** (Scheme 6). The instability of **M1′** versus **M′** could be attributed to four factors: (1) the relatively high oxidation state Rh(V), (2) less conjugation, (3) very rigid rhodacycle construction, and (4) the larger sterically repulsive interaction between the $-CH_2CH_2Ph$ and $-CH_3$ groups. To demonstrate the repulsive interaction, we replaced these two groups in **M1′** and **M′** with hydrogen atoms and found the energy difference between **M1′** and **M′** was reduced to 9.3 kcal/mol.

The reason that the ring opening from **L′** (path c) is an easy process while it is a difficult one from **H′** (path b) can be explained as follows. Rh(III) remained unchanged throughout

DOI: 10.1021/acs.joc.5b01895
J. Org. Chem. 2015, 80, 10686−10693

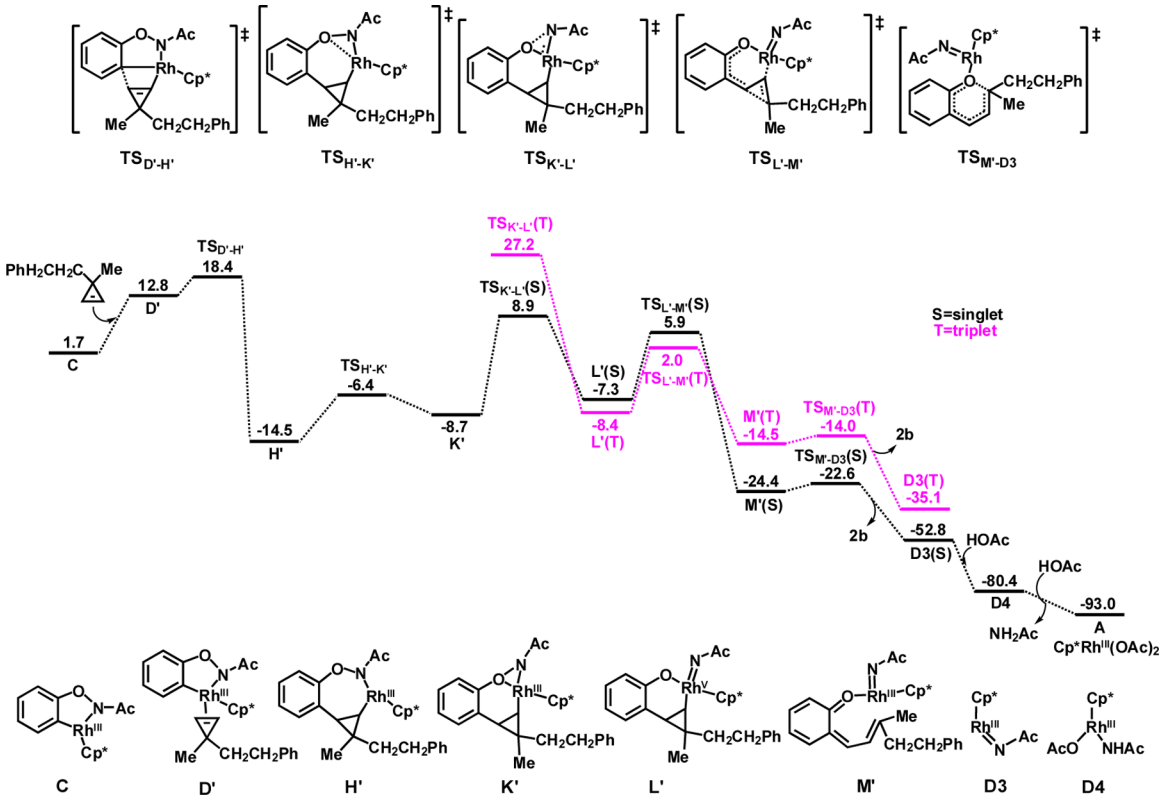

Figure 5. Energy profile calculated for **C** → **A** based on path c. The solvent-corrected free energies in the PCM model (MeOH as solvent) have been given in kcal/mol.

Scheme 6

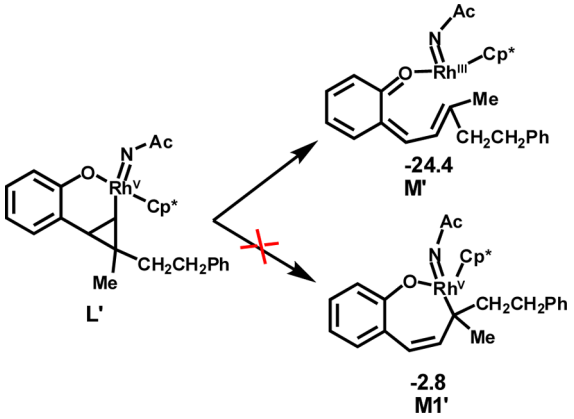

the path b, while path c proceeds via a Rh(V) species. It is obvious that the presence of the high oxidation state Rh(V) center in **L**′ (Figure 5) considerably facilitates the ring-opening process, while this is not the case for the ring opening from **H**′ (Figure 4). Furthermore, the NAc moiety in **H**′ eliminates the possibility of formation of a high conjugation structure after the ring opening from **H**′ as compared to **L**′.

The deprotonation of the amino group could precede the cleavage of the C−H bond for the formation of **C** (Figure S1). However, the pathway shown in Figure S1 would need to overcome energy barriers of 29.8 kcal/mol (CH_2Cl_2 as solvent for alkyne system) and 30.5 kcal/mol (MeOH as solvent for cyclopropene system), which are 10.0 and 10.3 kcal/mol higher than that of the pathway shown in Figure 1, respectively (ΔG = 19.8 kcal/mol for alkyne system and ΔG = 20.2 kcal/mol for cyclopropene system).

In summary, both internal oxidant and coupling partners play significant roles in making the Rh(III) → Rh (V) process feasible in Rh(III)-catalyzed C−H functionalization reactions (Scheme 7).[8a,18,20] The strong internal oxidant makes Rh(V) accessible and promotes a Rh(III)/Rh(V) catalytic cycle, while the weak internal oxidant favors reductive elimination prior to the oxidation. The alkene and cyclopropene coupling partners make it possible to access Rh(V).

4. CONCLUSIONS

The reaction mechanisms for the rhodium(III)-catalyzed C−H activation of *N*-phenoxyacetamide, in which the amido component of the internal oxidant serves as a leaving group, have been studied using the density functional M06 method. The first three steps of this mechanism were found to be similar for the alkyne and cyclopropene substrates, and involved sequential N−H deprotonation, C−H activation (a concerted metalation-deprotonation process), and alkyne insertion/cyclopropene double bond insertion. Starting from a seven-membered rhodacycle for alkyne sytem, our calculations supported a one-step concerted process in which the C−O bond-forming reductive elimination and O−N bond cleavage steps simultaneously occurred. Therefore, Rh(III) remained unchanged throughout the pathway for alkyne substrate.

Starting from a seven-membered rhodacycle for cyclopropene system, the reaction mechanisms were as follows: (1) the isomerization to form the Rh−O dative bond; (2) the formation of the Rh(V) nitrene complex through the cleavage of the O−N bond; (3) the ring-opening step via *β*-carbon elimination; and (4) the electrocyclization step to form the C−

DOI: 10.1021/acs.joc.5b01895
J. Org. Chem. 2015, 80, 10686−10693

Scheme 7

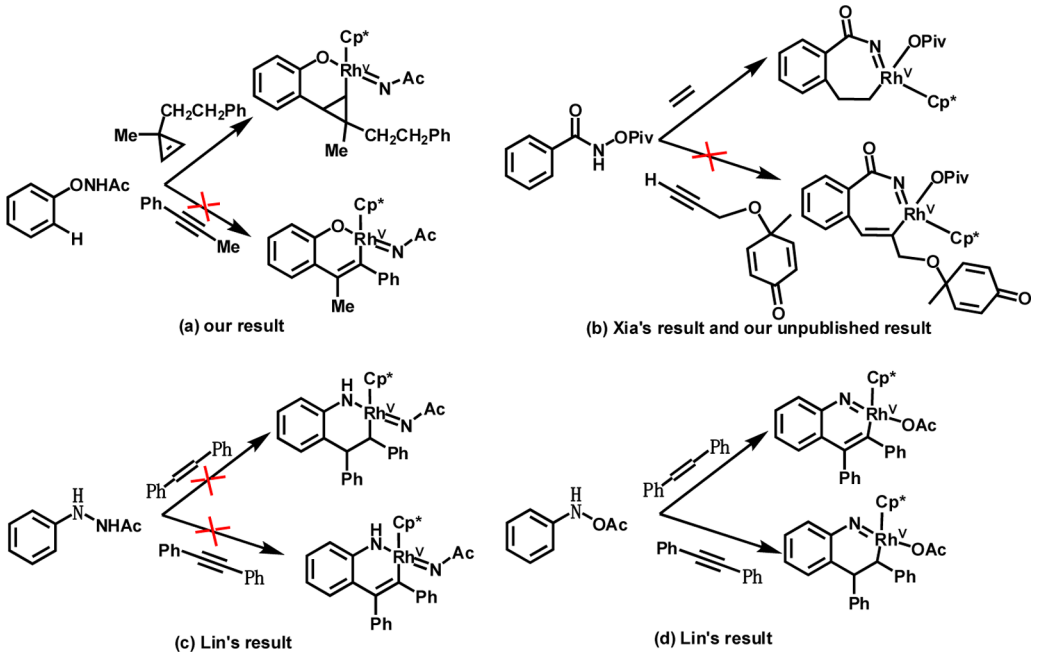

O bond. The energy profiles were accompanied by a change in the spin-state because the triplet spin state was found to be lower in energy than the singlet spin state for the Rh(V) nitrene complex.

■ ASSOCIATED CONTENT

Supporting Information

The Supporting Information is available free of charge on the ACS Publications website at DOI: 10.1021/acs.joc.5b01895.

Complete ref 17, calculated imaginary frequencies of all transition states species, and tables of Cartesian coordinates and electronic energies for all of the calculated structures (PDF)

■ AUTHOR INFORMATION

Corresponding Author

*E-mail: tchjli@jnu.edu.cn.

Notes

The authors declare no competing financial interest.

■ ACKNOWLEDGMENTS

This work was supported by the National Natural Science Foundation of China (Grant no. 21573095), the Fundamental Research Funds for the Central Universities (Grant no. 21615405), and the high-performance computing platform of Jinan University.

■ REFERENCES

(1) Reviews on Rh-catalyzed C−H activation: (a) Satoh, T.; Miura, M. *Chem. - Eur. J.* **2010**, *16*, 11212. (b) Wencel-Delord, J.; Droge, T.; Liu, F.; Glorius, F. *Chem. Soc. Rev.* **2011**, *40*, 4740. (c) Song, G.; Wang, F.; Li, X. *Chem. Soc. Rev.* **2012**, *41*, 3651. (d) Colby, D. A.; Bergman, R. G.; Ellman, J. A. *Chem. Rev.* **2010**, *110*, 624. (e) Kuhl, N.; Schroder, N.; Glorius, F. *Adv. Synth. Catal.* **2014**, *356*, 1443. (f) Wendlandt, A. E.; Suess, A. M.; Stahl, S. S. *Angew. Chem., Int. Ed.* **2011**, *50*, 11062. (g) Cho, S. H.; Kim, J. Y.; Kwak, J.; Chang, S. *Chem. Soc. Rev.* **2011**, *40*, 5068. (h) Arockiam, P. B.; Bruneau, C.; Dixneuf, P. H. *Chem. Rev.* **2012**, *112*, 5879.

(2) (a) Song, G.; Chen, D.; Pan, C.; Crabtree, R. H.; Li, X. *J. Org. Chem.* **2010**, *75*, 7487. (b) Su, Y.; Zhao, M.; Han, K.; Song, G.; Li, X. *Org. Lett.* **2010**, *12*, 5462. (c) Jayakumar, J.; Parthasarathy, K.; Cheng, C. *Angew. Chem., Int. Ed.* **2012**, *51*, 197. (d) Umeda, N.; Tsurugi, H.; Satoh, T.; Miura, M. *Angew. Chem., Int. Ed.* **2008**, *47*, 4019. (e) Shimizu, M.; Hirano, K.; Satoh, T.; Miura, M. *J. Org. Chem.* **2009**, *74*, 3478.

(3) (a) Mochida, S.; Hirano, K.; Satoh, T.; Miura, M. *J. Org. Chem.* **2009**, *74*, 6295. (b) Patureau, F. W.; Besset, T.; Glorius, F. *Angew. Chem., Int. Ed.* **2011**, *50*, 1064. (c) Liu, B.; Fan, Y.; Gao, Y.; Sun, C.; Xu, C.; Zhu, J. *J. Am. Chem. Soc.* **2013**, *135*, 468. (d) Zhen, W.; Wang, F.; Zhao, M.; Du, Z.; Li, X. *Angew. Chem., Int. Ed.* **2012**, *51*, 11819.

(4) (a) Xie, F.; Qi, Z.; Li, X. *Angew. Chem., Int. Ed.* **2013**, *52*, 11862. (b) Yang, Y.; Hou, W.; Qin, L.; Du, J.; Feng, H.; Zhou, B.; Li, Y. *Chem. - Eur. J.* **2014**, *20*, 416.

(5) For some examples of N−O bond cleavage, see: (a) Guimond, N.; Gouliaras, C.; Fagnou, K. *J. Am. Chem. Soc.* **2010**, *132*, 6908. (b) Guimond, N.; Gorelsky, S. I.; Fagnou, K. *J. Am. Chem. Soc.* **2011**, *133*, 6449. (c) Patureau, F. W.; Glorius, F. *Angew. Chem., Int. Ed.* **2011**, *50*, 1977. (d) Hyster, T. K.; Rovis, T. *Chem. Commun.* **2011**, *47*, 11846. (e) Neely, J. M.; Rovis, T. *J. Am. Chem. Soc.* **2013**, *135*, 66. (f) Huang, H.; Ji, X.; Wu, W.; Jiang, H. *Chem. Soc. Rev.* **2015**, *44*, 1155.

(6) For some examples of N−N bond cleavage, see: (a) Wang, C.; Sun, H.; Fang, Y.; Huang, Y. *Angew. Chem., Int. Ed.* **2013**, *52*, 5795. (b) Zhao, D.; Shi, Z.; Glorius, F. *Angew. Chem., Int. Ed.* **2013**, *52*, 12426. (c) Liu, B.; Song, C.; Sun, C.; Zhou, S.; Zhu, J. *J. Am. Chem. Soc.* **2013**, *135*, 16625. (d) Wang, C.; Huang, Y. *Org. Lett.* **2013**, *15*, 5294. (e) Chuang, S.; Gandeepan, P.; Cheng, C. *Org. Lett.* **2013**, *15*, 5750. (f) Huang, X.; Yang, X.; Song, R.; Li, J. *J. Org. Chem.* **2014**, *79*, 1025. (g) Zheng, L.; Hua, R. *Chem. - Eur. J.* **2014**, *20*, 2352. (h) Muralirajan, K.; Cheng, C. *Adv. Synth. Catal.* **2014**, *356*, 1571.

(7) (a) Liu, G.; Shen, Y.; Zhou, Z.; Lu, X. *Angew. Chem., Int. Ed.* **2013**, *52*, 6033. (b) Zhang, H.; Wang, K.; Wang, B.; Yi, H.; Hu, F.; Li, C.; Zhang, Y.; Wang, J. *Angew. Chem., Int. Ed.* **2014**, *53*, 13234. (c) Shen, Y.; Liu, G.; Zhou, Z.; Lu, X. *Org. Lett.* **2013**, *15*, 3366. (d) Hu, F.; Xia, Y.; Ye, F.; Liu, Z.; Ma, C.; Zhang, Y.; Wang, J. *Angew. Chem., Int. Ed.* **2014**, *53*, 1364. (e) Zhou, J.; Shi, J.; Liu, X.; Jia, J.; Song, H.; Xu, H.; Yi, W. *Chem. Commun.* **2015**, *51*, 5868.

(8) (a) Xu, L.; Zhu, Q.; Huang, G.; Cheng, B.; Xia, Y. *J. Org. Chem.* **2012**, *77*, 3017. (b) Park, S. H.; Kwak, J.; Shin, K.; Ryu, J.; Park, Y.; Chang, S. *J. Am. Chem. Soc.* **2014**, *136*, 2492. (c) Figg, T. M.; Park, S.; Park, J.; Chang, S.; Musaev, D. G. *Organometallics* **2014**, *33*, 4076.

DOI: 10.1021/acs.joc.5b01895
J. Org. Chem. 2015, 80, 10686−10693

(d) Collins, K. D.; Lied, F.; Glorius, F. *Chem. Commun.* **2014**, *50*, 4459. (e) Wang, H.; Schroder, N.; Glorius, F. *Angew. Chem., Int. Ed.* **2013**, *52*, 5386. (f) Ng, F. N.; Zhou, Z.; Yu, W. *Chem. - Eur. J.* **2014**, *20*, 4474. (g) Zhou, T.; Guo, W.; Xia, Y. *Chem. - Eur. J.* **2015**, *21*, 9209.
(9) Lorpitthaya, R.; Xie, Z.; Sophy, K. B.; Kuo, J.; Liu, X. *Chem. - Eur. J.* **2010**, *16*, 588.
(10) (a) Zhao, Y.; Schultz, N. E.; Truhlar, D. G. *J. Chem. Phys.* **2005**, *123*, 161103. (b) Zhao, Y.; Truhlar, D. G. *Acc. Chem. Res.* **2008**, *41*, 157. (c) Zhao, Y.; Truhlar, D. G. *Theor. Chem. Acc.* **2008**, *120*, 215. (d) Zhao, Y.; Truhlar, D. G. *J. Chem. Theory Comput.* **2009**, *5*, 324.
(11) (a) Fukui, K. *J. Phys. Chem.* **1970**, *74*, 4161. (b) Fukui, K. *Acc. Chem. Res.* **1981**, *14*, 363.
(12) (a) Hay, P. J.; Wadt, W. R. *J. Chem. Phys.* **1985**, *82*, 299. (b) Wadt, W. R.; P. Hay, P. J. *J. Chem. Phys.* **1985**, *82*, 284.
(13) Ehlers, A. W.; Böhme, M.; Dapprich, S.; Gobbi, A.; Höllwarth, A.; Jonas, V.; Köhler, K. F.; Stegmann, R.; Veldkamp, A.; Frenking, G. *Chem. Phys. Lett.* **1993**, *208*, 111.
(14) Hariharan, P. C.; Pople, J. A. *Theor. Chim. Acta.* **1973**, *28*, 213.
(15) (a) Barone, V.; Cossi, M. *J. Phys. Chem. A* **1998**, *102*, 1995. (b) Cossi, M.; Rega, N.; Scalmani, G.; Barone, V. *J. Comput. Chem.* **2003**, *24*, 669. (c) Tomasi, J.; Mennucci, B.; Cammi, R. *Chem. Rev.* **2005**, *105*, 2999.
(16) (a) Fuentealba, P.; Preuss, H.; Stoll, H.; Vonszentpaly, L. *Chem. Phys. Lett.* **1982**, *89*, 418. (b) Szentpaly, L. V.; Fuentealba, P.; Preuss, H.; Stoll, H. *Chem. Phys. Lett.* **1982**, *93*, 555. (c) Fuentealba, P.; Stoll, H.; Szentpaly, L. V.; Schwerdtfeger, P.; Preuss, H. *J. Phys. B: At. Mol. Phys.* **1983**, *16*, L323.
(17) Frisch, M. J.; et al. *Gaussian 09*, revision C.01; Gaussian, Inc.: Wallingford, CT, 2010. [Full reference given in the Supporting Information.]
(18) Chen, W.-J.; Lin, Z. *Organometallics* **2015**, *34*, 309.
(19) (a) Lin, X. F.; Zhao, C. Y.; Che, C. M.; Ke, Z.; Phillips, D. L. *Chem. - Asian J.* **2007**, *2*, 1101. (b) Pritchina, E. A.; Gritsan, N. P.; Bally, T.; Autrey, T.; Liu, Y.; Wang, Y.; Toscano, J. P. *Phys. Chem. Chem. Phys.* **2003**, *5*, 1010. (c) Pritchina, E. A.; Gritsan, N. P.; Bally, T. *Russ. Chem. Bull.* **2005**, *54*, 525.
(20) Du, L.; Li, J., unpublished results.

DOI: 10.1021/acs.joc.5b01895
J. Org. Chem. 2015, 80, 10686−10693